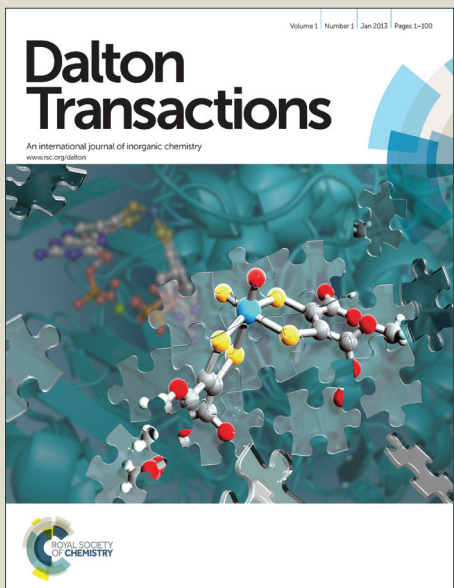


# Dalton Transactions

Accepted Manuscript



This is an Accepted Manuscript, which has been through the Royal Society of Chemistry peer review process and has been accepted for publication.

Accepted Manuscripts are published online shortly after acceptance, before technical editing, formatting and proof reading. Using this free service, authors can make their results available to the community, in citable form, before we publish the edited article. We will replace this Accepted Manuscript with the edited and formatted Advance Article as soon as it is available.

You can find more information about Accepted Manuscripts in the [Information for Authors](#).

Please note that technical editing may introduce minor changes to the text and/or graphics, which may alter content. The journal's standard [Terms & Conditions](#) and the [Ethical guidelines](#) still apply. In no event shall the Royal Society of Chemistry be held responsible for any errors or omissions in this Accepted Manuscript or any consequences arising from the use of any information it contains.

Cite this: DOI: 10.1039/c0xx00000x

www.rsc.org/xxxxxx

ARTICLE TYPE

## Catalytic Water Oxidation Based on Ag(I)-Substituted Keggin Polyoxotungstophosphate

Ying Cui,<sup>a</sup> Lei Shi,<sup>a</sup> Yanyi Yang,<sup>a</sup> Wansheng You,<sup>a\*</sup> Lancui Zhang,<sup>a</sup> Zaiming Zhu,<sup>a</sup> Meiyiing Liu,<sup>a</sup> and Licheng Sun<sup>\*b</sup>

Received (in XXX, XXX) Xth XXXXXXXXX 20XX, Accepted Xth XXXXXXXXX 20XX

DOI: 10.1039/b000000x

A 1D chain-like Ag(I)-substituted Keggin polyoxotungstophosphate,  $K_3[H_3Ag^I PW_{11}O_{39}] \cdot 12H_2O$ , has been synthesized in high yield and characterized by single-crystal X-ray diffraction, XRD, IR, TG/DTA and elemental analysis. When the polyoxotungstophosphate is dissolved in aqueous solutions, <sup>31</sup>P NMR, MS and conductivity indicate that a Ag(I) anion-complex formulated as  $[H_3Ag^I(H_2O)PW_{11}O_{39}]^{3-}$  is formed and it is stable in solution of pH 3.5-7.0. The oxidation of  $[H_3Ag^I(H_2O)PW_{11}O_{39}]^{3-}$  by  $S_2O_8^{2-}$  has been studied by ESR, UV-visible spectroscopy, <sup>31</sup>P NMR and UV-Raman spectroscopy. It is found that  $[H_3Ag^I(H_2O)PW_{11}O_{39}]^{3-}$  can be oxidized to generate a dark green Ag(II) anion-complex  $[H_3Ag^{II}(H_2O)PW_{11}O_{39}]^{2-}$  dominantly and a small amount of Ag(III) complex  $[H_3Ag^{III}OPW_{11}O_{39}]^{3-}$ , and evolving  $O_2$  simultaneously. Compared with  $[Ag^I(2,2'-bpy)NO_3]$  and  $AgNO_3$ ,  $[H_3Ag^I(H_2O)PW_{11}O_{39}]^{3-}$  has the higher activity in chemical water oxidation. This illustrates that the  $[PW_{11}O_{39}]^{7-}$  ligand plays important roles in both the transmission of electrons and protons, and the improvement of redox performance of silver ions. The rate of  $O_2$  evolution is a first-order law with respect to the concentrations of  $[H_3Ag^I(H_2O)PW_{11}O_{39}]^{3-}$  and  $S_2O_8^{2-}$ , respectively. A possible catalytic water oxidation mechanism of  $[H_3Ag^I(H_2O)PW_{11}O_{39}]^{3-}$  is proposed, in which the  $[H_3Ag^{II}(H_2O)PW_{11}O_{39}]^{2-}$  and  $[H_3Ag^{III}OPW_{11}O_{39}]^{3-}$  intermediates are determined and the rate-determining step is that  $[H_3Ag^{III}OPW_{11}O_{39}]^{3-}$  oxidizes water into  $H_2O_2$ .

### Introduction

Water oxidation into  $O_2$ , as a half-reaction, is the key step to sustainable energy systems including water splitting into  $H_2$  or direct conversion of carbon dioxide into methanol. In the last decades, a robust, fast and inexpensive water oxidation catalyst (WOC) has been being pursued.<sup>1-4</sup> Since Meyer and co-workers reported the ‘blue dimer’<sup>5</sup> *cis*, *cis*- $[(bpy)_2(H_2O)Ru^{III}ORu^{III}(H_2O)(bpy)_2]^{4+}$ , a range of homogeneous molecular catalysts of metal-organic complexes containing manganese, iron, cobalt, ruthenium, iridium, etc. have been reported successively,<sup>6-16</sup> and the catalytic activity and the chemical stability have been increased dramatically. In 2012, Sun et al.<sup>17</sup> reported a mononuclear ruthenium complex  $[Ru(bda)(isoq)_2]$  with high catalytic activity (TOF > 300  $s^{-1}$ ) and chemical stability (TON = 8,360 ± 91) for water oxidation, which is moderately comparable with the reaction rate of the oxygen-evolving complex of photosystem II *in vivo*.

For all homogenous WOCs with organic ligands reported to date, however, it is fatal that they are oxidatively deactivated. In recent years, polyoxometalates have been selected as inorganic ligands to be assembled into the catalysts because they possess the higher stability towards oxidative degradation.<sup>18</sup> As homogenous molecular WOCs, a series of ruthenium- and cobalt- polyoxometalate complexes, including  $[\{Ru_4O_4(OH)_2(H_2O)_4\}(\gamma-SiW_{10}O_{36})_2]^{10-19-25}$ ,  $[Ru^{III}(H_2O)XW_{11}O_{39}]^{5-}$  ( $X = Si$  and  $Ge$ ),<sup>26</sup>  $[\{Ru_3O_3(H_2O)Cl_2\}(SiW_9O_34)]^{27}$ ,  $[Co_4(H_2O)_2(\alpha-B-PW_9O_{34})_2]^{10-28-30}$ ,  $[Co_3O_2O_2H_6]^{3-31}$ ,  $[Co_2Mo_{10}O_{38}H_4]^{6-31}$ ,  $[Co^{III}Co^{II}(H_2O)W_{11}O_{39}]^{7-32}$  and  $Cs_{15}K[Co_9(H_2O)_6(OH)_7(HPO_4)_2(PW_9O_34)]$  (a heterogeneous catalyst),<sup>33</sup> have been reported. They exhibit high catalytic activity for water oxidation into  $O_2$  in photoinduced chemical oxidation and electrocatalytic oxidation systems. For example,  $[\{Ru_4O_4(OH)_2(H_2O)_4\}(\gamma-SiW_{10}O_{36})_2]^{10-}$  exhibits the peak catalytic performance of TOF > 450  $h^{-1}$  in chemical oxidation<sup>20</sup> and 306  $h^{-1}$  at  $\eta = 0.60$  V in electrochemical oxidation,<sup>25</sup> which exceeds the value of Co- and

Mn-systems based on organic ligands.<sup>34,35</sup>  $[Co_4(H_2O)_2(\alpha-B-PW_9O_{34})_2]^{10-30}$ , a sandwich tetracobalt complex based on  $[\alpha-B-PW_9O_{34}]^{9-}$  ligand, has received more attention because it consists of the earth abundant elements. As homogenous molecular catalysts, the stability of polyoxometalate complexes are more evident in the dispute of  $[Co_4(H_2O)_2(\alpha-B-PW_9O_{34})_2]^{10-60}$  between Hill<sup>36</sup> and Finke.<sup>37,38</sup> Therefore, polyoxometalates are no doubt one of promising ligands for developing homogenous molecular catalysts. In addition, polyoxometalate complexes, as molecular catalysts, are more suitable to elucidate the catalytic mechanism of water oxidation because of their stability and defined structures. Fukuzumi et al.<sup>26</sup> have proposed a catalytic mechanism of  $[Ru^{III}(H_2O)XW_{11}O_{39}]^{5-}$  ( $X = Si$  and  $Ge$ ), involving the multistep oxidation of Ru atoms and the formation of O–O bonds. Employing DFT calculation on the mechanism of the single-Ru-substituted polyoxometalates, Su et al.<sup>39</sup> have indicated that the polytungstate ligands act as the most favorable proton acceptor in the O–O bond formation, with an energy barrier of 28.43 kcal·mol<sup>-1</sup>. However, WOCs based on polyoxometalate ligand are only limited to Co(II) and Ru(III)/(IV) complexes. It would be interesting to develop polyoxometalate complex catalysts of other metal ions to date.

The Ag(I) ion is often used as a powerful catalyst for most  $S_2O_8^{2-}$  oxidation reactions.<sup>40</sup> It has ever been reported the kinetics and the mechanism of Ag(I)-catalyzed water oxidation into  $O_2$  by  $S_2O_8^{2-}$  in aqueous solution.<sup>40,41</sup> In 2012, Li et al.<sup>42</sup> prepared a Ag-based electrode which has favorable activity for  $O_2$  evolution and lower overpotential in mild conditions. To our knowledge, Ag(I) salts are the best homogenous molecular catalyst among simple inorganic salts, including  $Co^{2+}$ ,  $Mn^{2+}$ ,  $Ru^{3+}$ , etc. The catalytic activity could be improved by decorating central metal ions effectively by suitable ligands. However, organic ligands would capture radicals, one of efficient oxidizing agents, to lead to loss of catalytic activity of Ag(I).<sup>41</sup> It would be a good choice to develop efficient WOCs of Ag(I) complexes based on polyoxometalates as ligands. Based

on the considerations above, our attention has been focused on WOCs based on Ag(I)-polyoxometalate complexes.

## Results and Discussion

### Synthesis and Crystal Structure

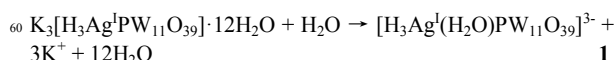
Employing  $\text{Na}_3[\text{A-PW}_9\text{O}_{34}] \cdot 7\text{H}_2\text{O}$  as the raw material, a Ag(I)-substituted Keggin polyoxotungstophosphate, the crystal of  $\text{K}_3[\text{H}_3\text{Ag}^{\text{I}}\text{PW}_{11}\text{O}_{39}] \cdot 12\text{H}_2\text{O}$ , has been synthesized in high yield. As shown in Table S1, it is isomorphic with  $\text{K}_3[\text{Ag}\text{PW}_{11}\text{O}_{39}] \cdot 9.25\text{H}_2\text{O} \cdot \text{CH}_3\text{OH}$  reported by Nogueira et al.<sup>[43]</sup> In the crystal structure, Ag(I) ions, exhibiting an eight-coordination fashion, bridge monolacunary  $\alpha$ -Keggin forming a one-dimensional anionic  $[\text{Ag}^{\text{I}}\text{PW}_{11}\text{O}_{39}]_{\text{n}}^{6-}$  chain (Fig. S1).<sup>43</sup>  $\text{K}^+$  ions, as counterions, are six-coordinated to oxygen atoms of  $[\text{Ag}^{\text{I}}\text{PW}_{11}\text{O}_{39}]^{6-}$  units and water molecules. The experimental and simulated PXRD patterns of  $\text{K}_3[\text{H}_3\text{Ag}^{\text{I}}\text{PW}_{11}\text{O}_{39}] \cdot 12\text{H}_2\text{O}$  are shown in Fig. S2. The diffraction peaks match well in key positions, indicating the crystal phase purity. For some peaks, the difference in intensity may be caused by the preferred orientation of the powder sample.

### Formation and Stability of $[\text{H}_3\text{Ag}^{\text{I}}(\text{H}_2\text{O})\text{PW}_{11}\text{O}_{39}]^{3-}$ in Aqueous Solution

When crystal of  $\text{K}_3[\text{H}_3\text{Ag}^{\text{I}}\text{PW}_{11}\text{O}_{39}] \cdot 12\text{H}_2\text{O}$  is dissolved in water, the solution is at pH *ca.* 5 (Table 1) and exhibits only one single  $^{31}\text{P}$  NMR signal at  $\delta = -11.00$  ppm (Fig. 1b-1e). -0.57 ppm signal in Fig. 1e is attributed to  $\text{Na}_2\text{HPO}_4\text{-NaH}_2\text{PO}_4$ . The only one signal illustrates that there is only one existential state of  $\{\text{PW}_{11}\text{O}_{39}\}$  ligand in the solution. Compared with  $^{31}\text{P}$  NMR of  $\text{PW}_{11}\text{O}_{39}^{7-}$  (Fig. 1a), it is found that the  $^{31}\text{P}$  NMR signal of the  $\text{K}_3[\text{H}_3\text{Ag}^{\text{I}}\text{PW}_{11}\text{O}_{39}] \cdot 12\text{H}_2\text{O}$  solution shifts negatively. This results from decreasing the interactions between the P atoms and the central O<sub>a</sub> atoms due to the introduction of Ag(I) ions into the lacunary sites of  $\text{PW}_{11}\text{O}_{39}^{7-}$ . This illustrates that a complex of  $\text{Ag}^+$  and  $\text{PW}_{11}\text{O}_{39}^{7-}$  is formed.

As shown in Fig. 2, a MS spectrum of  $\text{K}_3[\text{H}_3\text{Ag}^{\text{I}}\text{PW}_{11}\text{O}_{39}] \cdot 12\text{H}_2\text{O}$  solution exhibits several groups of  $m/z$  peaks in the range of 920–950. The main peak assignments are listed in Table S2. It is found that there are two complex anions:  $[\text{H}_3\text{Ag}^{\text{I}}\text{PW}_{11}\text{O}_{39}]^{3-}$  and  $[\text{H}_3\text{Ag}^{\text{I}}(\text{H}_2\text{O})\text{PW}_{11}\text{O}_{39}]^{3-}$ . However, the above-mentioned  $^{31}\text{P}$  NMR indicates that there may be only one polyoxotungstophosphate complex species in the solution. Which one? The  $^{31}\text{P}$  NMR chemical shift of  $\text{K}_3[\text{H}_3\text{Ag}^{\text{I}}\text{PW}_{11}\text{O}_{39}] \cdot 12\text{H}_2\text{O}$  in solution is identical with that in solid state<sup>43</sup>, which demonstrates that the distances between the lacunary O atoms and the Ag ion are not changed observably when it is dissolved. Therefore, the valence sum calculation of the solid state is used to determine which is the most probable complex in solution. For  $[\text{H}_3\text{Ag}^{\text{I}}\text{PW}_{11}\text{O}_{39}]^{3-}$ , the  $\text{Ag}^+$  is a tetra-coordinated configuration. The valence sum of the  $\text{Ag}^+$  is 0.855 (Table S3), which can not satisfy its valence. Therefore, it is deduced that the complex should be unstable in solution. Therefore, it may be generated in high temperature and electric field of MS analysis. For  $[\text{H}_3\text{Ag}^{\text{I}}(\text{H}_2\text{O})\text{PW}_{11}\text{O}_{39}]^{3-}$ , the valence sum of the  $\text{Ag}^+$  is 1.1712, which is closer to that in the solid state. This demonstrates that  $[\text{H}_3\text{Ag}^{\text{I}}(\text{H}_2\text{O})\text{PW}_{11}\text{O}_{39}]^{3-}$  is more stable in solution. Combined with the feature of substituted Keggin polyoxometalates,<sup>44</sup> therefore, it is deduced that  $[\text{H}_3\text{Ag}^{\text{I}}(\text{H}_2\text{O})\text{PW}_{11}\text{O}_{39}]^{3-}$  may be generated when  $\text{K}_3[\text{H}_3\text{Ag}^{\text{I}}\text{PW}_{11}\text{O}_{39}] \cdot 12\text{H}_2\text{O}$  is dissolved in aqueous solution (as

expressed in equation 1).



In order to further confirm the existence of  $[\text{H}_3\text{Ag}^{\text{I}}(\text{H}_2\text{O})\text{PW}_{11}\text{O}_{39}]^{3-}$ , the conductivity and the pH values have been measured for the aqueous solutions of  $65 \text{ K}_3[\text{H}_3\text{Ag}^{\text{I}}\text{PW}_{11}\text{O}_{39}] \cdot 12\text{H}_2\text{O}$ . As shown in Table 1, the degree of

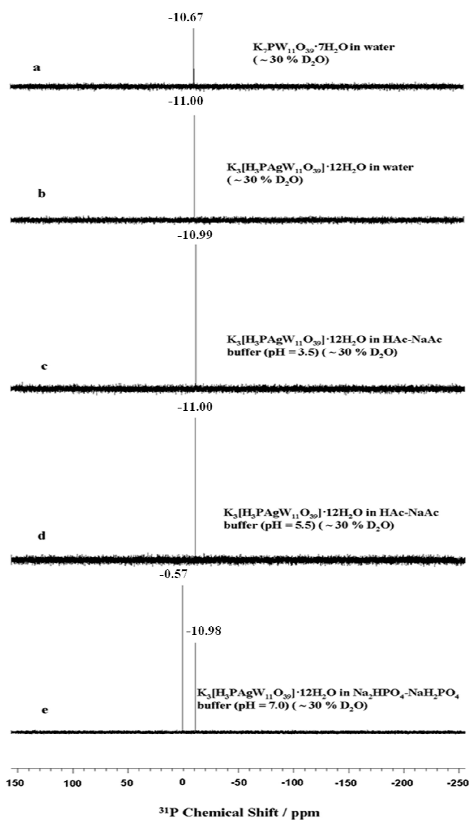


Fig. 1.  $^{31}\text{P}$  NMR spectra for solutions of a:  $\text{K}_3[\text{Ag}^{\text{I}}\text{PW}_{11}\text{O}_{39}] \cdot 12\text{H}_2\text{O}$  in pure water; b:  $\text{K}_3[\text{Ag}^{\text{I}}\text{PW}_{11}\text{O}_{39}] \cdot 12\text{H}_2\text{O}$  in pure water (~30%  $\text{D}_2\text{O}$ ); c:  $\text{K}_3[\text{Ag}^{\text{I}}\text{PW}_{11}\text{O}_{39}] \cdot 12\text{H}_2\text{O}$  in  $\text{HAc-NaAc}$  buffer (pH = 3.5); d:  $\text{K}_3[\text{Ag}^{\text{I}}\text{PW}_{11}\text{O}_{39}] \cdot 12\text{H}_2\text{O}$  in  $\text{HAc-NaAc}$  buffer (pH = 5.5); e:  $\text{K}_3[\text{Ag}^{\text{I}}\text{PW}_{11}\text{O}_{39}] \cdot 12\text{H}_2\text{O}$  in  $\text{Na}_2\text{HPO}_4\text{-NaH}_2\text{PO}_4$  buffer (pH = 7.0)

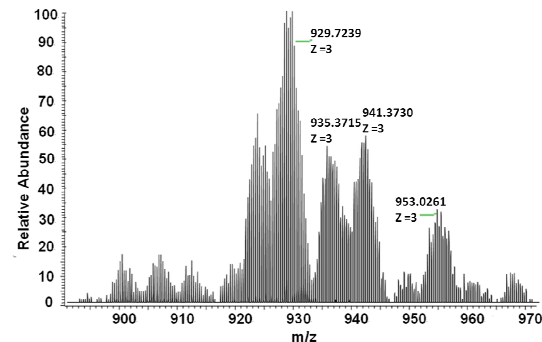


Fig. 2. Mass spectra for  $\text{K}_3[\text{Ag}^{\text{I}}\text{PW}_{11}\text{O}_{39}] \cdot 12\text{H}_2\text{O}$  solution

$\text{H}^+$  ion dissociation and its estimated  $K_a$  are  $\sim 0.1\%$  and  $\sim 10^{-9}$  for the concentrations of 0.010–0.002 M respectively. This illustrates that the  $\text{H}^+$  ion dissociation in

Cite this: DOI: 10.1039/c0xx00000x

www.rsc.org/xxxxxx

## ARTICLE TYPE

$[\text{H}_3\text{Ag}^{\text{I}}(\text{H}_2\text{O})\text{PW}_{11}\text{O}_{39}]^{3-}$  is very little and its contribution to the conductivity can be negligible. The molar conductivity values are in the range of  $400\text{-}450 \text{ s} \cdot \text{m}^2 \cdot \text{mol}^{-1}$ , indicating that the

number of dissociated ions is 4 and the corresponding compound is the  $\text{M}_3\text{A}$  model.<sup>45</sup> It is confirmed that the above conclusion is reasonable.

**Table 1.** Conductivity and  $K_a$  of  $\text{K}_3[\text{H}_3\text{Ag}^{\text{I}}(\text{H}_2\text{O})\text{PW}_{11}\text{O}_{39}] \cdot 12\text{H}_2\text{O}$  solutions<sup>a</sup>

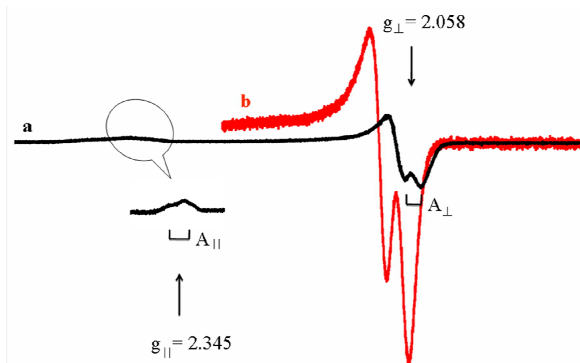
Concentration (M)	Conductivity K (S/cm)	Molar conductivity $\Lambda_m (\text{S} \cdot \text{m}^2 \cdot \text{mol}^{-1})^b$	pH	$[\text{H}^+]$ (M)	Degree of $\text{H}^+$ dissociation (%)	$K_a^c$
0.010	$0.40 \times 10^4$	400	5.16	$6.9 \times 10^{-6}$	0.069	$4.7 \times 10^{-9}$
0.008	$0.32 \times 10^4$	400	5.22	$6.0 \times 10^{-6}$	0.075	$4.5 \times 10^{-9}$
0.006	$0.25 \times 10^4$	417	5.30	$5.0 \times 10^{-6}$	0.084	$4.2 \times 10^{-9}$
0.004	$1.70 \times 10^3$	425	5.38	$4.2 \times 10^{-6}$	0.104	$4.4 \times 10^{-9}$
0.002	$0.90 \times 10^3$	450	5.52	$3.0 \times 10^{-6}$	0.150	$4.5 \times 10^{-9}$

<sup>a</sup> Solution temperature: 18 °C; <sup>b</sup>  $\Lambda_m = K \times 10^{-3}/C$ ; <sup>c</sup>  $K_a = [\text{H}^+]^2/C$ 

In order to determine the stability of  $[\text{H}_3\text{Ag}^{\text{I}}(\text{H}_2\text{O})\text{PW}_{11}\text{O}_{39}]^{3-}$  in aqueous solutions at different pH values,  $^{31}\text{P}$  NMR of  $[\text{H}_3\text{Ag}^{\text{I}}(\text{H}_2\text{O})\text{PW}_{11}\text{O}_{39}]^{3-}$  solutions have been measured in pH = 3.5, 5.5 and 7.0 buffers (Fig. 1c-e). Only one single  $^{31}\text{P}$  NMR signal is also observed and kept at  $\delta = -11.00$  ppm. It illustrates that  $[\text{H}_3\text{Ag}^{\text{I}}(\text{H}_2\text{O})\text{PW}_{11}\text{O}_{39}]^{3-}$  is stable in pH 3.5-7.0 solutions.

**Oxidation of  $[\text{H}_3\text{Ag}^{\text{I}}(\text{H}_2\text{O})\text{PW}_{11}\text{O}_{39}]^{3-}$** 

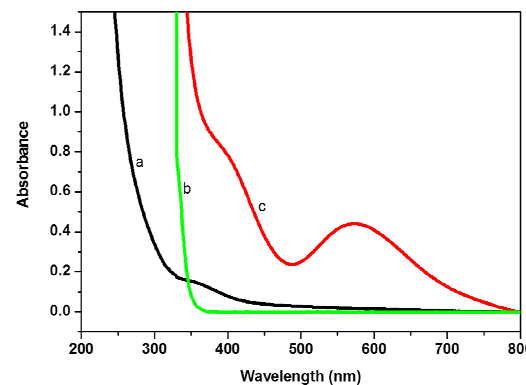
As reported,  $\text{S}_2\text{O}_8^{2-}$  has been used to oxidize the coordinated metal ion into high oxidation state in metal ions (Mn, Am, Tb and Pr)-substituted polyoxotungstates, where lacunary polyoxometalate anions are used to stabilize the high oxidation states of coordinated metal ions.<sup>46-49</sup> In our work, when an excess of  $\text{Na}_2\text{S}_2\text{O}_8$  is added to a colourless  $[\text{H}_3\text{Ag}^{\text{I}}(\text{H}_2\text{O})\text{PW}_{11}\text{O}_{39}]^{3-}$  solution, a dark green solution is formed. What is the dark green species?

**Fig. 3.** ESR spectra of solutions of a:  $\text{Na}_2\text{S}_2\text{O}_8$  (0.26 M) +  $\text{K}_3[\text{H}_3\text{Ag}^{\text{I}}(\text{H}_2\text{O})\text{PW}_{11}\text{O}_{39}] \cdot 12\text{H}_2\text{O}$  ( $5.76 \times 10^{-3}$  M) and b:  $\text{Na}_2\text{S}_2\text{O}_8$  ( $8.8 \times 10^{-2}$  M) +  $\text{AgNO}_3$  ( $1.18 \times 10^{-3}$  M) at 100 K. UV-visible Spectra of Oxidation of  $[\text{H}_3\text{Ag}^{\text{I}}(\text{H}_2\text{O})\text{PW}_{11}\text{O}_{39}]^{3-}$ 

**ESR Analysis of Oxidation of  $[\text{H}_3\text{Ag}^{\text{I}}(\text{H}_2\text{O})\text{PW}_{11}\text{O}_{39}]^{3-}$ .** In order to determine oxidation state of Ag ions after the oxidation of  $[\text{H}_3\text{Ag}^{\text{I}}(\text{H}_2\text{O})\text{PW}_{11}\text{O}_{39}]^{3-}$  by  $\text{S}_2\text{O}_8^{2-}$ , we have carried out *in situ* ESR spectroscopy of the solutions of  $\text{Na}_2\text{S}_2\text{O}_8 + \text{K}_3[\text{H}_3\text{Ag}^{\text{I}}(\text{H}_2\text{O})\text{PW}_{11}\text{O}_{39}] \cdot 12\text{H}_2\text{O}$  and  $\text{Na}_2\text{S}_2\text{O}_8 + \text{AgNO}_3$  at 100 K. As shown in Fig. 3a, markedly anisotropic g factors ( $g_{\parallel} = 2.345$  and  $g_{\perp} = 2.058$ ) and the anisotropic doublet hyperfine splittings ( $A_{\parallel} = 44.1 \text{ G}$  and  $A_{\perp} = 23.1 \text{ G}$ ) obtained from the solution of  $\text{Na}_2\text{S}_2\text{O}_8 + \text{K}_3[\text{H}_3\text{Ag}^{\text{I}}(\text{H}_2\text{O})\text{PW}_{11}\text{O}_{39}] \cdot 12\text{H}_2\text{O}$  agree well with those of

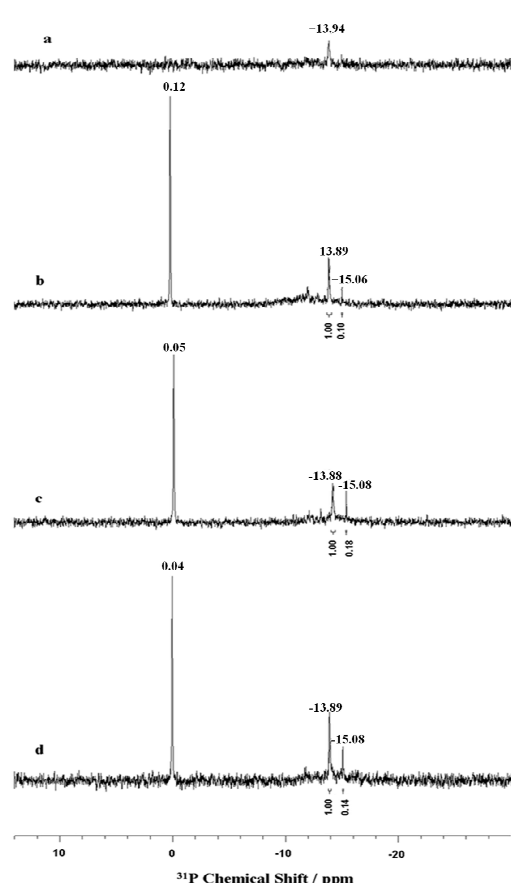
the divalent silver ions.<sup>51-55</sup> Compared with ESR spectrum of the  $\text{Na}_2\text{S}_2\text{O}_8 + \text{AgNO}_3$  solution (Fig. 3b), the spectra are similar in fashion, but the corresponding parameters are not identical because Ag(II) ions are located in different coordinated environments. This illustrates that the Ag(I) ions in  $[\text{H}_3\text{Ag}^{\text{I}}(\text{H}_2\text{O})\text{PW}_{11}\text{O}_{39}]^{3-}$  are oxidized into Ag(II) ions.

**UV-visible Spectra of Oxidation of  $[\text{H}_3\text{Ag}^{\text{I}}(\text{H}_2\text{O})\text{PW}_{11}\text{O}_{39}]^{3-}$ .** The UV-Visible spectra are recorded for (a)  $\text{AgNO}_3$ , (b)  $\text{K}_7[\text{PW}_{11}\text{O}_{39}] \cdot 12\text{H}_2\text{O}$  (c)  $\text{K}_3[\text{H}_3\text{Ag}^{\text{I}}(\text{H}_2\text{O})\text{PW}_{11}\text{O}_{39}] \cdot 12\text{H}_2\text{O}$  in phosphate buffer solution (pH = 5.5) containing  $\text{Na}_2\text{S}_2\text{O}_8$  (Fig. 4). For the solution of  $\text{AgNO}_3$  and  $\text{Na}_2\text{S}_2\text{O}_8$ , only one band at 370 nm is observed, which is attributed to Ag(III).<sup>50</sup> (Fig. 4a). No absorption is observed in the region of 800-400 nm. For the solution of  $\text{K}_7[\text{PW}_{11}\text{O}_{39}] \cdot 12\text{H}_2\text{O}$  and  $\text{Na}_2\text{S}_2\text{O}_8$  no absorption is also observed in the region of 800-350 nm. (Fig. 4b) However, for solution of  $\text{Na}_2\text{S}_2\text{O}_8$  and  $\text{K}_3[\text{H}_3\text{Ag}^{\text{I}}(\text{H}_2\text{O})\text{PW}_{11}\text{O}_{39}] \cdot 12\text{H}_2\text{O}$ , it is noted that two strong absorbance bands appear at 408 and 582 nm (Fig. 4c). Based on the position of bands and the result of ESR, it is reasonably deduced that the band at 582 nm corresponds to the electron transition of  $^2\text{E}_g \rightarrow ^2\text{T}_{2g}$  of Ag(II) in an approximate six-coordinated environment and the band at 408 nm is

**Fig. 4.** UV-Visible spectra of solutions of a:  $7.0 \times 10^{-3}$  M  $\text{AgNO}_3$  and  $8.8 \times 10^{-2}$  M  $\text{Na}_2\text{S}_2\text{O}_8$ ; b:  $6.0 \times 10^{-3}$  M  $\text{K}_7[\text{PW}_{11}\text{O}_{39}] \cdot 12\text{H}_2\text{O}$  and  $8.8 \times 10^{-2}$  M  $\text{Na}_2\text{S}_2\text{O}_8$ ; c:  $6.0 \times 10^{-3}$  M  $\text{K}_3[\text{H}_3\text{Ag}^{\text{I}}(\text{H}_2\text{O})\text{PW}_{11}\text{O}_{39}] \cdot 12\text{H}_2\text{O}$  and  $8.8 \times 10^{-2}$  M  $\text{Na}_2\text{S}_2\text{O}_8$

attributed to the absorbance of Ag(III). Therefore, it is deduced that  $[H_3Ag^I(H_2O)PW_{11}O_{39}]^{3-}$  may be oxidized by  $S_2O_8^{2-}$ , generating  $[H_3Ag^{II}(H_2O)PW_{11}O_{39}]^{2-}$  and  $[H_3Ag^{III}OPW_{11}O_{39}]^{3-}$ .

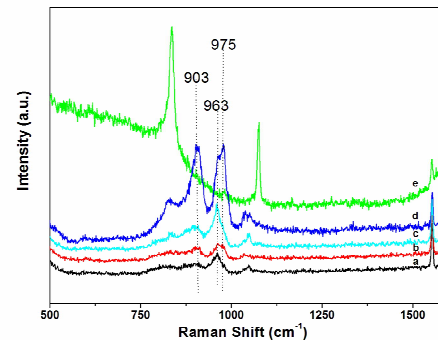
**5  $^{31}P$  NMR of Oxidation of  $[H_3Ag^I(H_2O)PW_{11}O_{39}]^{3-}$ .** After an excess of  $Na_2S_2O_8$  is added to the aqueous solution of  $[H_3Ag^I(H_2O)PW_{11}O_{39}]^{3-}$ , the  $^{31}P$  NMR signal of  $[H_3Ag^I(H_2O)PW_{11}O_{39}]^{3-}$  at -11.00 ppm disappears and a new single  $^{31}P$  NMR signal at -13.9 ppm appears (Fig. 5a). To our knowledge, the upfield  $^{31}P$  NMR chemical shift may result from two possible causes: polymerization of  $[PW_{11}O_{39}]^{7-}$  into  $[P_2W_{21}O_{71}]^{6-}$  or  $[PW_{12}O_{40}]^{3-}$ , or oxidation Ag(I) into Ag(II) or Ag(III). Solution of  $[PW_{11}O_{39}]^{7-}$  is stable between pH 2 and 6 and even in the presence of  $S_2O_8^{2-}$ .<sup>45-48</sup> The condition in which 15 the former reaction occurs should have acidified  $[H_3Ag^I(H_2O)PW_{11}O_{39}]^{3-}$  solution. In order to exclude the former cause, a phosphate buffer solution of pH 5.5 is carried out. It is found that the chemical shift of -13.9 ppm is also kept (Fig. 5b-d). 20 0.12 signals in Fig. 5b-d are attributed to  $Na_2HPO_4$  and  $NaH_2PO_4$ . The buffer solution remains the acidity of the solution unchanged in the process of oxidation reaction so that the polymerization reaction is not possible. If either  $[PW_{11}O_{39}]^{7-}$  was degraded or oxidized into polyperoxotungastophosphates,



25 **Fig. 5.**  $^{31}P$  NMR spectra for a solution of  $K_3[H_3Ag^I(H_2O)PW_{11}O_{39}] \cdot 12H_2O$  and excess of  $Na_2S_2O_8$ . a: In pure water; In 0.01 M phosphate buffer solution (pH = 5.5), data were collected three times at one hour intervals, b: 0 hour; c: 1 hours; d: 2 hours

30 they should have led to the downfield and multiple  $^{31}P$  NMR chemical shifts. Therefore, considering that only one  $^{31}P$  NMR signal at -13.9 ppm appears in the solution of  $Na_2S_2O_8$  and  $[H_3Ag^I(H_2O)PW_{11}O_{39}]^{3-}$ , it is inferred that the structure of the  $[PW_{11}O_{39}]^{7-}$  ligand should be remained unchanged during the 35 oxidation reaction. The upfield  $^{31}P$  NMR chemical shift in oxidation of  $[H_3Ag^I(H_2O)PW_{11}O_{39}]^{3-}$  should result from the increase of the oxidative state of the Ag atom due to the enhanced interaction between the Ag ions and the central  $O_a$  atoms, which had been observed in oxidation of  $[Ce^{III}(PW_{11}O_{39})_2]^{11-}$  into  $[Ce^{IV}(PW_{11}O_{39})]^{3-}$ .<sup>56</sup> Combined with the ESR and UV-Visible spectra mentioned above, it is reasonable that  $[H_3Ag^I(H_2O)PW_{11}O_{39}]^{3-}$  is oxidized by  $S_2O_8^{2-}$  into a Ag(II) complex (equation 2). In addition, it is found that the oxidation of  $[H_3Ag^I(H_2O)PW_{11}O_{39}]^{3-}$  into  $[H_3Ag^{II}(H_2O)PW_{11}O_{39}]^{2-}$  is fast and almost complete under the experimental conditions.

In a phosphate buffer solution, as shown in Fig. 5, the chemical shift of  $\delta \sim -13.9$  ppm with a relative intensity of 1.00 is not only kept, but also a new weak signal at  $\delta = -15.06 \sim -15.08$  ppm with a relative intensity of 0.10 ~ 0.18 emerges. This shows that  $[H_3Ag^{II}(H_2O)PW_{11}O_{39}]^{2-}$  exists dominantly in the reaction system, and another intermediate species, with very low concentration, may be formed. It has ever been reported<sup>43</sup> that Ag(III) ions may exist as  $AgO^+$  in solution.<sup>57-59</sup> Allen et al.<sup>58</sup> have estimated by free energy data that equilibrium constant K (25 °C) is *ca.*  $2.2 \times 10^{-4}$  for the equation  $(2Ag^{2+} + H_2O = AgO^+ + Ag^+ + 2H^+)$ . Therefore, it is deduced that a small amount of  $[H_3Ag^{II}(H_2O)PW_{11}O_{39}]^{2-}$  may be oxidized into a Ag(III) complex species,  $[H_3Ag^{III}(O)PW_{11}O_{39}]^{3-}$ . The reaction is 60 described as equation 4. The amount of  $[H_3Ag^{III}OPW_{11}O_{39}]^{3-}$  depends on the pH in the solutions. As the concentration of  $[H_3Ag^{III}OPW_{11}O_{39}]^{3-}$  is increased in pH 5.5 buffer solution, the weak  $^{31}P$  NMR signal at  $\delta = -15.06 \sim -15.08$  ppm appears. In pure water solution, the low pH value caused by the oxidation 65 reactions inhibits the formation of  $[H_3Ag^{III}OPW_{11}O_{39}]^{3-}$  so that the  $^{31}P$  NMR signal would not be observed.



70 **Fig. 6.** UV-Raman spectra for 0.01 M solutions of a:  $K_7[PW_{11}O_{39}] \cdot 12H_2O$ , b:  $K_3[H_3AgPW_{11}O_{39}] \cdot 12H_2O$ , c:  $K_7[PW_{11}O_{39}] \cdot 12H_2O$  and  $Na_2S_2O_8$ , d:  $K_3[H_3AgPW_{11}O_{39}] \cdot 12H_2O$  and  $Na_2S_2O_8$ , e:  $Na_2S_2O_8$ . Excited light source: 257 nm

#### UV-Raman Spectra of Oxidation of $[H_3Ag^I(H_2O)PW_{11}O_{39}]^{3-}$ .

75 Fig. 6 shows UV-Raman spectra for the solutions of  $K_7[PW_{11}O_{39}] \cdot 12H_2O$ ,  $K_3[H_3AgPW_{11}O_{39}] \cdot 12H_2O$ ,  $K_7[PW_{11}O_{39}] \cdot 12H_2O$  and  $Na_2S_2O_8$ ,  $K_3[H_3AgPW_{11}O_{39}] \cdot 12H_2O$  and  $Na_2S_2O_8$ ,  $Na_2S_2O_8$ . Excited light source: 257 nm

Cite this: DOI: 10.1039/c0xx00000x

www.rsc.org/xxxxxx

## ARTICLE TYPE

and  $\text{Na}_2\text{S}_2\text{O}_8$  as well as  $\text{Na}_2\text{S}_2\text{O}_8$ . For the solution of  $\text{K}_7[\text{PW}_{11}\text{O}_{39}] \cdot 12\text{H}_2\text{O}$ , the peaks at 963(m) and 903(w)  $\text{cm}^{-1}$  are observed, which are attributed to of the W(P)-O bond vibrations of the lacunary  $[\text{PW}_{11}\text{O}_{39}]^{7-}$  anion. When  $\text{Ag}^+$  ions are coordinated to the lacunary sites of  $[\text{PW}_{11}\text{O}_{39}]^{7-}$ , forming  $[\text{H}_3\text{Ag}^1(\text{H}_2\text{O})\text{PW}_{11}\text{O}_{39}]^{3-}$ , it is found that the peak at 903  $\text{cm}^{-1}$  is enhanced obviously and a new shoulder peak at 975  $\text{cm}^{-1}$  appears, which results from improving the symmetry of the polyoxotungstophosphate structure and decreasing its negative charge to some extent when a  $\text{Ag}^+$  ion is coordinated to the lacunary site of  $[\text{PW}_{11}\text{O}_{39}]^{7-}$ . When an excess of  $\text{S}_2\text{O}_8^{2-}$  is added to the  $[\text{PW}_{11}\text{O}_{39}]^{7-}$  solution, the peaks at 963 and 903  $\text{cm}^{-1}$  are still kept, but their seemingly enhanced intensity results from the absorption of  $\text{S}_2\text{O}_8^{2-}$ . Therefore, it is deduced that the UV-Raman peaks of  $[\text{PW}_{11}\text{O}_{39}]^{7-}$  should be fixed because the structure of  $[\text{PW}_{11}\text{O}_{39}]^{7-}$  is kept unchanged in the solution containing  $\text{S}_2\text{O}_8^{2-}$ .<sup>45-48</sup> However, when an excess of  $\text{S}_2\text{O}_8^{2-}$  is added to the  $[\text{H}_3\text{Ag}^1(\text{H}_2\text{O})\text{PW}_{11}\text{O}_{39}]^{3-}$  solution, the peaks at 963, 903 and 975  $\text{cm}^{-1}$  are enhanced obviously. This shows that the  $[\text{PW}_{11}\text{O}_{39}]^{7-}$  ligand is stable and the central  $\text{Ag}^+$  ion in the complex is oxidized into Ag(II) or Ag(III). This is consistent with the result of  $^{31}\text{P}$  NMR for oxidation of  $[\text{H}_3\text{Ag}^1(\text{H}_2\text{O})\text{PW}_{11}\text{O}_{39}]^{3-}$  solution.

#### Homogenous Catalytic Water Oxidation into $\text{O}_2$ for $[\text{H}_3\text{Ag}^1(\text{H}_2\text{O})\text{PW}_{11}\text{O}_{39}]^{3-}$

As known, the pure  $\text{S}_2\text{O}_8^{2-}$  solution is stable dynamically and no  $\text{O}_2$  evolution is almost observed at room temperature. In recent years, the  $\text{S}_2\text{O}_8^{2-}$  ion has been used as a two-electron oxidizing agent to evaluate the activity of WOCs.<sup>15,19,22,27,29-32</sup> To ensure that  $[\text{H}_3\text{Ag}^1(\text{H}_2\text{O})\text{PW}_{11}\text{O}_{39}]^{3-}$  is not decomposed, the catalytic water oxidation is carried out in a phosphate buffer solution (1 M, pH = 5.5) at 25 °C to keep pH values at 3.5-7.0. Isotope-labelling water oxidation experiments using  $^{18}\text{O}$  enriched water (8.3%) instead of  $\text{H}_2^{16}\text{O}$  were carried out with the catalyst to determine if the water is the source of the evolved oxygen. EI mass spectra of the gas sample evolved from the catalytic

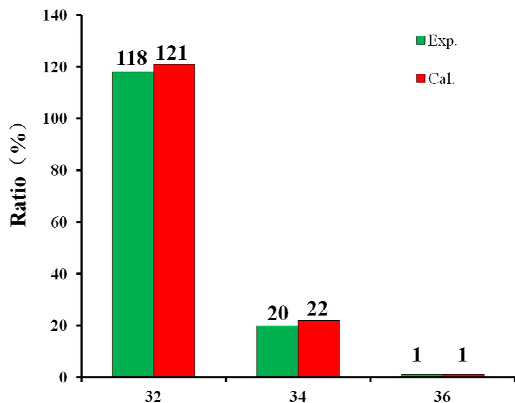


Fig. 7. Observed and theoretical relative abundances of  $^{18}\text{O}$ -labeled and unlabeled oxygen evolved during the photocatalytic oxidation of a buffer solution (12 mL) prepared with  $\text{H}_2^{18}\text{O}$ -enriched water (8.3%  $\text{H}_2^{18}\text{O}$ ) containing  $\text{K}_3[\text{H}_3\text{Ag}^1\text{PW}_{11}\text{O}_{39}] \cdot 12\text{H}_2\text{O}$  ( $2.0 \times 10^{-3}$  M) and  $\text{Na}_2\text{S}_2\text{O}_8$  ( $8.8 \times 10^{-2}$  M). (green, observed mass intensity; red, calculated values assuming that evolved  $\text{O}_2$  results exclusively from water).

oxidation in normal water and  $\text{H}_2^{18}\text{O}$ -enriched water (8.3%  $\text{H}_2^{18}\text{O}$ ) are shown in Fig. S7 and Fig. S8. The relative abundance of oxygen isotopes, which were determined from the intensities of those three molecular ion peaks, is listed on Fig. 7. The ratio of  $^{16}\text{O}^{16}\text{O} : ^{16}\text{O}^{18}\text{O} : ^{18}\text{O}^{18}\text{O}$  is determined to be 118:20:1, which is in good agreement with the simulated ratio of 121:22:1 for oxygen coming exclusively from water. The above data clearly demonstrates that the evolved  $\text{O}_2$  originates exclusively from the water, which is consistent with the results reported by the references<sup>32</sup>.

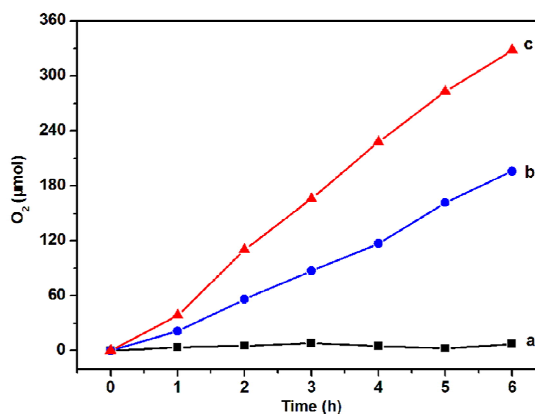


Fig. 8. Time course of  $\text{O}_2$  evolution from 100 ml of  $8.8 \times 10^{-2}$  M  $\text{Na}_2\text{S}_2\text{O}_8$  solution containing  $1.0 \times 10^{-3}$  M of a:  $[\text{Ag}(2,2'\text{-bpy})\text{NO}_3]$ ; b:  $\text{AgNO}_3$  and c:  $\text{K}_3[\text{H}_3\text{Ag}^1\text{PW}_{11}\text{O}_{39}] \cdot 12\text{H}_2\text{O}$  in 1 M phosphate buffer solution (pH = 5.5) at 25 °C.

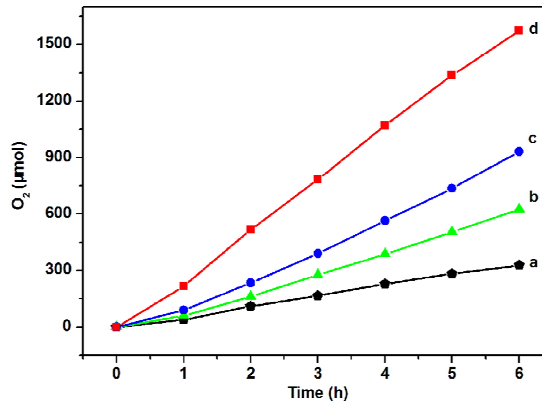


Fig. 9. Time course of  $\text{O}_2$  evolution from 100 ml of  $8.8 \times 10^{-2}$  M  $\text{Na}_2\text{S}_2\text{O}_8$  solution containing different concentrations of  $[\text{H}_3\text{Ag}^1(\text{H}_2\text{O})\text{PW}_{11}\text{O}_{39}] \cdot 12\text{H}_2\text{O}$  in 1 M phosphate buffer solution (pH = 5.5) at 25 °C. a:  $1.0 \times 10^{-3}$  M; b:  $2.0 \times 10^{-3}$  M; c:  $3.0 \times 10^{-3}$  M and d:  $5.0 \times 10^{-3}$  M.

Firstly, the catalytic activity of  $\text{K}_3[\text{H}_3\text{Ag}^1\text{PW}_{11}\text{O}_{39}] \cdot 12\text{H}_2\text{O}$ ,  $[\text{Ag}^1(2,2'\text{-bpy})\text{NO}_3]$ <sup>42</sup> and  $\text{AgNO}_3$  are compared. As shown in Fig. 8, no  $\text{O}_2$  evolution is observed for  $[\text{Ag}^1(2,2'\text{-bpy})\text{NO}_3]$ . For both  $\text{AgNO}_3$  and  $\text{K}_3[\text{H}_3\text{Ag}^1\text{PW}_{11}\text{O}_{39}] \cdot 12\text{H}_2\text{O}$ , however, obvious  $\text{O}_2$  evolution has been detected, and the amount of  $\text{O}_2$  comes to 196 and 328  $\mu\text{mol}$  in 6 hours, respectively. For the  $\text{K}_3[\text{H}_3\text{Ag}^1\text{PW}_{11}\text{O}_{39}] \cdot 12\text{H}_2\text{O}$  catalyst, the obviously increasing of  $\text{O}_2$  evolution illustrates that  $[\text{PW}_{11}\text{O}_{39}]^{7-}$  ligand plays a significant role in both the transmission of electrons and protons

and the improvement of the redox performance of the active Ag centers.

As shown in Fig. 9, the rates of  $O_2$  evolution increase with the increasing concentrations of  $[H_3Ag^I(H_2O)PW_{11}O_{39}]^{3-}$ . For 1.0, 2.0, 3.0 and 5.0 mM  $[H_3Ag^I(H_2O)PW_{11}O_{39}]^{3-}$ , the amount of  $O_2$  evolution comes to 328, 622, 935, 1575  $\mu\text{mol}$  in 6 hours, respectively. It is also found in Fig. 9 that the amount of  $O_2$  evolution in the first hour is lower relatively, especially for 3.0 and 5.0 mM concentrations, which may be an induced period of the oxidation process of  $[H_3Ag^I(H_2O)PW_{11}O_{39}]^{3-}$  into  $[H_3Ag^{II}(H_2O)PW_{11}O_{39}]^{2-}$ . This process is also observed by UV spectra (Fig. S4). Therefore, the kinetics of  $O_2$  evolution is

investigated in the time range of the second to the sixth hour. Within this time range the amount of  $O_2$  evolution vs the time exhibits an excellent linear relationship (Fig. 9). The rates of  $O_2$  evolution from systems with different concentrations of  $S_2O_8^{2-}$  and  $[H_3Ag^I(H_2O)PW_{11}O_{39}]^{3-}$  in 1 M phosphate buffer solution ( $\text{pH} = 5.5$ ) at 25 °C are listed in Table 2.

It is obvious that the rate of  $O_2$  evolution is a first-order law with respect to the concentrations of  $[H_3Ag^I(H_2O)PW_{11}O_{39}]^{3-}$  and  $S_2O_8^{2-}$ , respectively. The rate equation can be described as follows:

$$dc(O_2)/dt = kc([H_3Ag^I(H_2O)PW_{11}O_{39}]^{3-}) \cdot c(S_2O_8^{2-}) \quad 5$$

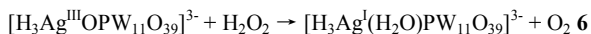
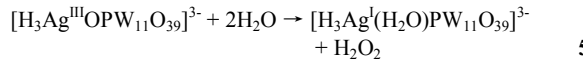
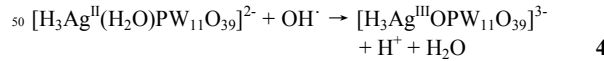
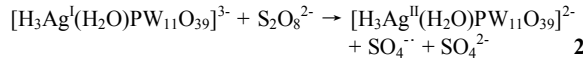
**Table 2.** Kinetics analysis of the rates of  $O_2$  evolution from systems with different concentrations of  $S_2O_8^{2-}$  and  $[H_3Ag^I(H_2O)PW_{11}O_{39}]^{3-}$  in 1 M phosphate buffer solution ( $\text{pH} = 5.5$ ) at 25 °C.

No.	$c([H_3Ag^I(H_2O)PW_{11}O_{39}]^{3-})$ ( $\text{mol} \cdot \text{L}^{-1}$ )	$c([S_2O_8^{2-}])^a$ ( $\text{mol} \cdot \text{L}^{-1}$ )	$v_m(O_2)^b$ ( $\mu\text{mol} \cdot \text{h}^{-1}$ )	$v(O_2)^c$ ( $\text{mol} \cdot \text{L}^{-1} \cdot \text{h}^{-1}$ )	$k$ ( $\text{L} \cdot \text{mol}^{-1} \cdot \text{h}^{-1}$ )	$k$ ( $\text{L} \cdot \text{mol}^{-1} \cdot \text{h}^{-1}$ )
1	$1.0 \times 10^{-3}$	$8.8 \times 10^{-2}$	55.2	$5.5 \times 10^{-4}$	62.7	
2	$1.0 \times 10^{-3}$	$17.6 \times 10^{-2}$	109.2	$1.1 \times 10^{-3}$	62.1	
3	$2.0 \times 10^{-3}$	$4.4 \times 10^{-2}$	54.4	$5.4 \times 10^{-4}$	61.8	
4	$2.0 \times 10^{-3}$	$8.8 \times 10^{-2}$	115.8	$1.2 \times 10^{-3}$	65.8	63.1
5	$3.0 \times 10^{-3}$	$8.8 \times 10^{-2}$	174.3	$1.7 \times 10^{-3}$	65.9	
6	$5.0 \times 10^{-3}$	$8.8 \times 10^{-2}$	267.0	$2.7 \times 10^{-3}$	60.7	

<sup>a</sup>  $c([S_2O_8^{2-}])$  is equal to initial concentration of  $S_2O_8^{2-}$  approximately. <sup>b</sup>  $v_m(O_2)$  represents the average rate of  $O_2$  evolution during the second to the sixth hour in the 100 ml solution and the values are a slope of a curve of the amount of  $O_2$  evolution vs time. <sup>c</sup>  $v(O_2)$  represents the rate of  $O_2$  evolution per volume of the solution and the values are  $v_m(O_2)/0.1 \text{ L}$ .

<sup>25</sup> The average rate constant at 25 °C is  $63.1 \times 10^6 \text{ L} \cdot \text{mol}^{-1} \cdot \text{h}^{-1}$ .

For the solutions of  $[H_3Ag^I(H_2O)PW_{11}O_{39}]^{3-}$  containing an excess of  $S_2O_8^{2-}$ , the noteworthy experimental evidences should be mentioned in the view of catalytic mechanism. Firstly, <sup>31</sup>P NMR indicates that there are  $[H_3Ag^{II}(H_2O)PW_{11}O_{39}]^{2-}$  and  $[H_3Ag^{III}OPW_{11}O_{39}]^{3-}$ , but no  $[H_3Ag^I(H_2O)PW_{11}O_{39}]^{3-}$  in the solutions. This demonstrates that the oxidation reaction of  $[H_3Ag^I(H_2O)PW_{11}O_{39}]^{3-}$  into  $[H_3Ag^{II}(H_2O)PW_{11}O_{39}]^{2-}$  and  $[H_3Ag^{III}OPW_{11}O_{39}]^{3-}$  is a fast reaction, not a rate-determining step for water oxidation into  $O_2$  evolution. Secondly, the organic substances ( $CH_3COO^-$ , 2,2-bipy, etc.) quench the  $O_2$  evolution owing to their competition of free radicals with the oxidation of  $[H_3Ag^{II}(H_2O)PW_{11}O_{39}]^{2-}$ . This also demonstrates that free radicals participate in water oxidation into  $O_2$ . Thirdly, the rate of  $O_2$  evolution is a first-order law with respect to the concentrations of  $[H_3Ag^I(H_2O)PW_{11}O_{39}]^{3-}$  and  $S_2O_8^{2-}$ , respectively. Finally, our recent result of catalytic water oxidation of  $AgNO_3$  indicates that the reaction ( $AgO^+ + H_2O \rightarrow Ag^+ + H_2O_2$ ) may be the rate-determined step.<sup>60</sup> Based on the aforementioned evidences, a possible mechanism of catalytic water oxidation into  $O_2$  evolution for  $[H_3Ag^I(H_2O)PW_{11}O_{39}]^{3-}$  is proposed:



<sup>55</sup> Among them, equation 5, the formation of  $O_2$  evolution, is a rate-determining step. The result is different from the catalytic mechanism of simple  $Ag(I)$  ions proposed by Kimura et al., in which the step ( $Ag^+ + S_2O_8^{2-} \rightarrow Ag^{2+} + SO_4^- + SO_4^{2-}$ ) was considered as a rate-determining reaction of  $O_2$  evolution.<sup>41</sup>

<sup>60</sup> Applying the steady-state approximation to the aforementioned mechanism, a theoretical rate equation is deduced as follows:

$$dc(O_2)/dt = kc([H_3Ag^I(H_2O)PW_{11}O_{39}]^{3-})c(S_2O_8^{2-}) \quad 7$$

It is consistent with the effects of the concentrations of  $[H_3Ag^I(H_2O)PW_{11}O_{39}]^{3-}$  and  $S_2O_8^{2-}$  on the rate of  $O_2$  evolution in the kinetic experiment.

In order to test the stability of the catalyst, we have performed the catalytic reaction for  $5.0 \times 10^{-5} \text{ M}$  of  $K_3[H_3Ag^I(H_2O)PW_{11}O_{39}] \cdot 12H_2O$  and  $AgNO_3$ . As shown in Fig. S9, it is found that the TON values are 95.0 and 66.0 in 96 hours respectively. The catalytic oxidation reaction is still undergoing with the high rate of  $O_2$  evolution.

## Experimental Section

### Materials and Methods

<sup>75</sup> All chemicals were commercially purchased and used as supplied.  $Na_9[A-PW_9O_{34}] \cdot 7H_2O$ ,<sup>61</sup>  $K_7[a-PW_{11}O_{39}] \cdot 12H_2O$ <sup>62</sup> and  $[Ag(2,2'-bipy)NO_3]$ <sup>63</sup> were synthesized according to the corresponding references and identified by IR spectroscopy. The content of K, P, Ag and W elements was determined by ICP-<sup>80</sup> PRODIGY XP analysis. IR spectra were recorded in the range of 400-4000  $\text{cm}^{-1}$  on a TENSOR27 Bruker AXS spectrometer

Cite this: DOI: 10.1039/c0xx00000x

www.rsc.org/xxxxxx

## ARTICLE TYPE

with a pressed KBr pellet. TG-DTA analyses were carried out on a Pyris Diamond TG/DTA instrument in immobile airflow from 30 to 900 °C with a heating rate of 10 °C·min<sup>-1</sup>. H<sub>2</sub>O molecules in crystal were determined according to TG analysis result. Powder X-ray diffraction measurement was collected on a D8 Advance instrument in the angular range of  $2\theta = 5\text{--}60^\circ$  at 293 K with Cu  $K\alpha$  radiation. MS analysis was performed on LTQ Orbitrap XL equipped with an ESI source. The following mass spectrometric conditions were used for the analysis in negative ion electrospray mode: Ispray voltage, 4.00 kV; Sheath gas flow rate, 30 arb; Aux gas flow rate, 10 arb; Capillary temperature, 275.00 °C. The conductivity was measured by a DDS-11A conductometer, using redistilled water. pH values were measured by Cyberscan 510 pH meter, using redistilled water.<sup>10</sup> <sup>31</sup>P NMR spectra were recorded on Bruker AVANCE500 spectrometer at 11.75 T using D<sub>2</sub>O locking field. <sup>31</sup>P chemical shifts were referenced to 85 % H<sub>3</sub>PO<sub>4</sub>. ESR signals at 100 K were recorded on a Bruker ESR A 200 spectrometer. The settings for the ESR spectrometer were as follows: center field, 3275.00 G; sweep width, 2000 G; microwave frequency, 9.43 GHz; modulation frequency, 100 kHz; power, 20.32 mW. UV-Visible spectra were obtained by a UV-240 UV-Vis spectrophotometer with the conditions: scan rate, 100 nm/min; wavenumber, 800-200 nm.

**25 Synthesis and Characteristic of K<sub>3</sub>[H<sub>3</sub>Ag<sup>I</sup>PW<sub>11</sub>O<sub>39</sub>]·12H<sub>2</sub>O**

5.0 ml of silver nitrate solution (0.26 g, 1.5 mmol) was added to 30 ml of Na<sub>9</sub>[A-PW<sub>9</sub>O<sub>34</sub>]·7H<sub>2</sub>O solution (2.56 g, 1.0 mmol). The resulting solution was adjusted to pH = 5.0 using 6 M HNO<sub>3</sub>. After 3 hours, the little amount of white precipitate was filtered off and 2.0 g KNO<sub>3</sub> were added to the filtered mother-liquor. After one day, white acicular crystals of K<sub>3</sub>[H<sub>3</sub>Ag<sup>I</sup>PW<sub>11</sub>O<sub>39</sub>]·12H<sub>2</sub>O were obtained in a yield of 70 % (based on Na<sub>9</sub>[PW<sub>9</sub>O<sub>34</sub>]·7H<sub>2</sub>O). Found: K, 3.89 %; P, 1.00 %; W, 64.56 %; Ag, 3.51 %. Calc. for K<sub>3</sub>H<sub>27</sub>AgO<sub>51</sub>PW<sub>11</sub>: K, 3.76 %; P, 0.99 %; W, 64.78 %; Ag, 3.45 %. Characteristic bands in the FT-IR spectrum of 955 cm<sup>-1</sup>, 904, 859, 808 and 730 cm<sup>-1</sup>; 1046 and 1090 cm<sup>-1</sup> are assigned to v<sub>as</sub>(W=O), v<sub>as</sub>(W—O—W) and v<sub>as</sub>(P—O) respectively (Fig. S5), confirming its presence as a lacunary  $\alpha$ -Keggin polyoxotungstophosphate. TG/DTA analysis was shown in Fig. S6. From 30 to 480 °C, the total weight loss is 7.60 %, which attributed to the loss of absorption water, coordinated water and constitution water.

**Single-crystal X-ray Diffraction**

The crystal data of K<sub>3</sub>[H<sub>3</sub>Ag<sup>I</sup>PW<sub>11</sub>O<sub>39</sub>]·12H<sub>2</sub>O were collected on a SMART APEX II-CCD X-ray single crystal diffractometer at 293 K with graphite-monochromatic Mo  $K\alpha$  radiation ( $\lambda = 0.71073 \text{ \AA}$ ). The structure was solved by direct method and refined by full-matrix least squares method on F<sup>2</sup> using the SHELXS-97 software.<sup>64</sup> The H<sup>+</sup> ions in polyoxometalates were determined according to the research results in aqueous solution and in need of the charge balance. A summary of the crystallographic data was shown in Table S1. The selected bond lengths and angles of K<sub>3</sub>[H<sub>3</sub>Ag<sup>I</sup>PW<sub>11</sub>O<sub>39</sub>]·12H<sub>2</sub>O are listed in Table S4. The CSD number: 427568. Further details of the crystal structure investigation may be obtained from Fachinformationszentrum Karlsruhe, 76344 Eggenstein-

Leopoldshafen, Germany (fax: +49-7247-808-666; e-mail: [crysdata@fiz-karlsruhe.de](mailto:crysdata@fiz-karlsruhe.de); [http://www.fiz-karlsruhe.de/request\\_for\\_deposited\\_data.html](http://www.fiz-karlsruhe.de/request_for_deposited_data.html).)

**60 Catalytic Water Oxidation into O<sub>2</sub>**

The catalytic activity was examined in a self-made closed 500 ml Quartz reaction cell with 100 ml of 1 M phosphate buffer (pH = 5.5) solution. The reaction was carried out in Ar atmosphere. The amount of the produced O<sub>2</sub> was analyzed using gas chromatography (with a thermal conductivity detector and an Ar carrier).

**18O Isotope-labeled experiment**

12.0 ml of Na<sub>2</sub>HPO<sub>4</sub>-NaH<sub>2</sub>PO<sub>4</sub> buffer (1 M pH = 5.5) containing 8.3 atom% H<sub>2</sub><sup>18</sup>O, K<sub>3</sub>[H<sub>3</sub>Ag<sup>I</sup>PW<sub>11</sub>O<sub>39</sub>]·12H<sub>2</sub>O ( $2.0 \times 10^{-3}$  M) and Na<sub>2</sub>S<sub>2</sub>O<sub>8</sub> ( $8.8 \times 10^{-2}$  M) was deaerated with N<sub>2</sub> in a 100ml flask that was sealed with a rubber septum. After 6 h, 20  $\mu$ L of gas sample was drawn using a gas-tight syringe for gas analysis. A HP Series 6890 model chromatograph interfaced with a HP Series 5973 model mass spectrometer operating in electron impact ionization mode was used to collect the mass spectrometry data. The MS detector was tuned for maximum sensitivity (quadrupole temperature, 150 °C; ion source temperature, 230 °C, an He carrier). The single ion mode was used to scan for the ions m/z = 29, 32, 34, 36. Ions in the m/z 80 range 29 to 50 were also scanned in order to observe the abundance change of <sup>16</sup>O<sup>18</sup>O and <sup>18</sup>O<sup>18</sup>O, which evolved from H<sub>2</sub><sup>16</sup>O and H<sub>2</sub><sup>18</sup>O, respectively. The total flow rate into the spectrometer was limited to 1 mL/min. The GC was equipped with a molecular sieve column (30 m  $\times$  0.25 mm  $\times$  0.25  $\mu$ m), and the vaporizing chamber temperature and column temperature was set for 200 °C and 35 °C, respectively.

**Conclusions**

- When the crystal of K<sub>3</sub>[H<sub>3</sub>Ag<sup>I</sup>PW<sub>11</sub>O<sub>39</sub>]·12H<sub>2</sub>O is dissolved in water, the [H<sub>3</sub>Ag<sup>I</sup>(H<sub>2</sub>O)PW<sub>11</sub>O<sub>39</sub>]<sup>3-</sup> anion is formed and keeps stable in the pH range of 3.5-7.0. This illustrates that the lacunary polyoxometalates are excellent inorganic ligands, which can be coordinated with Ag<sup>+</sup> ions to generate stable complexes.
- It is determined that [H<sub>3</sub>Ag<sup>I</sup>(H<sub>2</sub>O)PW<sub>11</sub>O<sub>39</sub>]<sup>3-</sup> is oxidized by S<sub>2</sub>O<sub>8</sub><sup>2-</sup> into [H<sub>3</sub>Ag<sup>II</sup>(H<sub>2</sub>O)PW<sub>11</sub>O<sub>39</sub>]<sup>2-</sup> dominantly and a small amount of [H<sub>3</sub>Ag<sup>III</sup>OPW<sub>11</sub>O<sub>39</sub>]<sup>3-</sup>. This illustrates that lacunary polyoxometalates play an important role in stabilizing high-oxidation states of silver ions.
- [H<sub>3</sub>Ag<sup>I</sup>(H<sub>2</sub>O)PW<sub>11</sub>O<sub>39</sub>]<sup>3-</sup> is a better catalyst for S<sub>2</sub>O<sub>8</sub><sup>2-</sup> oxidizing water into O<sub>2</sub>. It illustrates that the [PW<sub>11</sub>O<sub>39</sub>]<sup>7-</sup> ligand plays important roles in both the transmission of electrons and protons, and the improvement of redox performance of silver ions.
- A possible catalytic mechanism is proposed. In the oxidation reaction, the [H<sub>3</sub>Ag<sup>II</sup>(H<sub>2</sub>O)PW<sub>11</sub>O<sub>39</sub>]<sup>2-</sup> and [H<sub>3</sub>Ag<sup>III</sup>OPW<sub>11</sub>O<sub>39</sub>]<sup>3-</sup> intermediates are determined and the rate-determining step is that [H<sub>3</sub>Ag<sup>III</sup>OPW<sub>11</sub>O<sub>39</sub>]<sup>3-</sup> oxidizes water into H<sub>2</sub>O<sub>2</sub>. The rate law is a first order with concentrations of [H<sub>3</sub>Ag<sup>I</sup>(H<sub>2</sub>O)PW<sub>11</sub>O<sub>39</sub>]<sup>3-</sup> and S<sub>2</sub>O<sub>8</sub><sup>2-</sup> respectively.

## Acknowledgements

We thank the National Science Foundation of China (No. 20773057), the State Key Laboratory of Fine Chemicals of China (KF 1204) and Key Laboratory of Polyoxometalates Science of Ministry of Education of China for support of this research.

## Notes and references

<sup>a</sup> Institute of Chemistry for Functionalized Materials, Liaoning Normal University, Dalian 116029, P. R. China. Fax: +86 411 82156858; Tel: +86 411 82159378; E-mail: wsyou@lnnu.edu.cn

<sup>b</sup> State Key Laboratory of Fine Chemicals, Dalian University of Technology, Dalian 116024, P. R. China. E-mail: sunlc@dlut.edu.cn

† Electronic Supplementary Information (ESI) available: structural diagram of  $[H_3AgPW_{11}O_{39}]^{3-}$ ; XRD patterns, IR, TG/DTD, Crystallographic data and selected bond lengths and angles of  $K_3[H_3AgPW_{11}O_{39}] \cdot 12H_2O$ ; the isotopic patterns at  $m/z = 935.3751$  for MS analysis of  $K_3[H_3AgPW_{11}O_{39}] \cdot 12H_2O$  solution; UV-visible spectra of the  $[H_3AgPW_{11}O_{39}]^{3-}$  and  $S_2O_8^{2-}$  solution. For ESI and CIF or other electronic format see 10.1039/b000000x/

1 M. G. Walter, E. L. Warren, J. R. Mekone, S. W. Boettcher, Q. X. Mi, E. A. Santori, N. S. Lewis, *Chem. Rev.*, 2010, **110**, 6446.

2 X. Sala, I. Romero, M. Rodriguez, L. Escriche, A. Llobet, *Angew. Chem. Int. Ed.*, 2009, **48**, 2842.

3 H. Yamazaki, A. Shouji, M. Kajita, M. Yagi, *Coord. Chem. Rev.*, 2010, **254**, 2483.

4 R. Brimblecombe, G. C. Dismukes, G. F. Swiegers, L. Spiccia, *Dalton Trans.*, 2009, 9374.

5 S. W. Gersten, G. J. Samuels, T. J. Meyer, *J. Am. Chem. Soc.*, 1982, **104**, 4029.

6 J. J. Concepcion, M. K. Tsai, J. T. Muckerman, T. J. Meyer, *J. Am. Chem. Soc.*, 2010, **132**, 1545.

7 J. Nyhén, L. L. Duan, B. Akermark, L. C. Sun, T. Privalov, *Angew. Chem. Int. Ed.*, 2010, **49**, 1773.

8 X. Sala, I. Romero, M. Rodríguez, L. Escriche, A. Llobet, *Angew. Chem. Int. Ed.*, 2009, **48**, 2842.

9 R. Zong, R. P. Thummel, *J. Am. Chem. Soc.*, 2005, **127**, 12802.

10 S. W. Kohl, L. Weiner, L. Schwartsbord, L. Konstantinovski, L. J. W. Shimon, Y. Ben-David, M. A. Iron, D. Milstein, *Science*, 2009, **324**, 74.

11 N. D. McDaniel, F. J. Coughlin, L. L. Tinker, S. Bernhard, *J. Am. Chem. Soc.*, 2008, **130**, 210.

12 H. Kunkely, A. Vogler, *Angew. Chem. Int. Ed.*, 2009, **48**, 1685.

13 J. Limburg, J. S. Vretos, J. M. LiableSands, A. L. Rheingold, R. H. Crabtree, G. W. Brudvig, *Science*, 1999, **283**, 1524.

14 W. C. Ellis, N. D. McDaniel, S. Bernhard, T. J. Collins, *J. Am. Chem. Soc.*, 2010, **132**, 10990.

15 Y. H. Xu, L. L. Duan, L. P. Tong, B. Akermarkb, L. C. Sun, *Chem. Commun.*, 2010, **46**, 6506.

16 M. Yagi, K. Narita, *J. Am. Chem. Soc.*, 2004, **126**, 8084.

17 L. L. Duan, F. Bozoglian, S. Mandal, B. Stewart, T. Privalov, A. Llobet, L. C. Sun, *Nat. Chem.*, 2012, **4**, 418.

18 H. Lv, Y. V. Geletii, C. Zhao, J. W. Vickers, G. Zhu, Z. Luo, J. Song, T. Lian, D. G. Musaev, C. L. Hill, *Chem. Soc. Rev.*, 2012, **41**, 7572.

19 Y. V. Geletii, B. Botar, P. Kogerler, D. A. Hillesheim, D. G. Musaev, C. L. Hill, *Angew. Chem. Int. Ed.*, 2008, **47**, 3896.

20 A. Sartorel, M. Carraro, G. Scorrano, R. D. Zorzi, S. Geremia, N. D. McDaniel, S. Bernhard, M. Bonchio, *J. Am. Chem. Soc.*, 2008, **130**, 5006.

21 M. Orlandi, R. Argazzi, A. Sartorel, M. Carraro, G. Scorrano, M. Bonchio, F. Scandola, *Chem. Commun.*, 2010, **46**, 3152.

22 Y. V. Geletii, Z. Q. Huang, Y. Hou, D. G. Musaev, T. Q. Lian, C. L. Hill, *J. Am. Chem. Soc.*, 2009, **131**, 7522.

23 Y. V. Geletii, C. Besson, Y. Hou, Q. S. Yin, D. G. Musaev, D. Quiñonero, R. Cao, K. I. Hardcastle, A. Proust, P. Kögerler, C. L. Hill, *J. Am. Chem. Soc.*, 2009, **131**, 17360.

24 A. Sartorel, P. Miró, E. Salvadori, S. Romain, M. Carraro, G. Scorrano, M. D. Valentín, A. Llobet, C. Bo, M. Bonchio, *J. Am. Chem. Soc.*, 2009, **131**, 16051.

25 F. M. Toma, A. Sartorel, M. Iurlo, M. Carraro, P. Parisse, C. Maccato, S. Rapino, B. R. Gonzalez, H. Amenitsch, T. D. Ros, L. Casalis, A. Goldoni, M. Marcaccio, G. Scorrano, G. Scoles, F. Paolucci, M. Pratol, M. Bonchio, *Nature Chem.*, 2010, **2**, 826.

26 M. Murakami, D. Hong, T. Suenobu, S. Yamaguchi, T. Ogura, S. Fukuzumi, *J. Am. Chem. Soc.*, 2011, **133**, 11605.

27 P. Car, M. Guttentag, K. K. Baldridge, R. Alberto, G. R. Patzk, *Green Chem.*, 2012, **14**, 1680.

28 Q. Yin, J. M. Tan, C. Besson, Y. V. Geletii, D. G. Musaev, A. E. Kuznetsov, Z. Luo, K. I. Hardcastle, C. L. Hill, *Science*, 2010, **328**, 342.

29 Z. Q. Huang, Z. Luo, Y. V. Geletii, J. W. Vickers, Q. S. Yin, D. Wu, Y. Hou, Y. Ding, J. Song, D. G. Musaev, C. L. Hill, T. Q. Lian, *J. Am. Chem. Soc.*, 2011, **133**, 2068.

30 M. Natali, S. Berardi, A. Sartorel, M. Bonchio, S. Campagnac, F. Scandola, *Chem. Commun.*, 2012, **48**, 8808.

31 S. Tanaka, M. Annaka, K. Sakai, *Chem. Commun.*, 2012, **48**, 1653.

32 F. Y. Song, Y. Ding, B. C. Ma, C. M. Wang, Q. Wang, X. Q. Du, S. Fu, J. Song, *Energy Environ. Sci.*, 2013, **6**, 1170.

33 J. Soriano-López, S. Goberna-Ferrón, L. Vigara, J. J. Carbó, J. M. Poblet, *Inorg. Chem.*, 2013, **52**, 4753.

34 M. K. Kanan, D. G. Nocera, *Science*, 2008, **321**, 1072.

35 M. J. Mas-Marza, E. Sala, X. Romero, I. Rodríguez, M. Viñas, C. Parella, T. Llobet, *Angew. Chem. Int. Ed.*, 2008, **47**, 5830.

36 J. W. Vickers, H. Lv, J. M. Sumliner, G. Zhu, Z. Luo, D. G. Musaev, Y. V. Geletii, C. L. Hill, *J. Am. Chem. Soc.*, 2013, **135**, 14110.

37 J. J. Stracke, R. G. Finke, *J. Am. Chem. Soc.*, 2011, **133**, 14872.

38 J. J. Stracke, R. G. Finke, *Catal.*, 2013, **3**, 1209.

39 Z. L. Lang, G. C. Yang, N. N. Ma, S. Z. Wen, L. K. Yan, W. Guan, Z. M. Su, *Dalton Trans.*, 2013, **42**, 10617.

40 D. A. House, *Chem. Rev.*, 1962, **62**, 185.

41 M. Kimura, T. Kawajiri, J. C. S. Dalton, 1980, 726.

42 W. Wang, Q. Zhao, X. J. Deng, J. P. Li, *J. Hydro. Energy*, 2011, **36**, 7374.

43 H. I. S. Nogueira, F. A. A. Paz, P. A. F. Teixeira, J. Klinowsk, *Chem. Commun.*, 2006, 2953.

44 M. T. Pope, *Heteropoly and isopoly oxometalates*, Springer-Verlag Berlin, 1983.

45 Z. Ma, *Experimental methods of applied inorganic chemistry*, Higher Education Press, 1991.

46 I. A. Weinstock, *Chem. Rev.*, 1998, **98**, 113.

47 X. Y. Zhang, M. T. Pope, M. R. Chance, G. B. Jameson, *Polyhedron*, 1995, **14**, 1381.

48 W. You, Y. Gu, *Chin. Chem. Lett.*, 1993, **4**, 369-370.

49 G. A. Ayoko, J. F. Iyun, I. F. El-Idris, *Transition Met. Chem.*, 1992, **17**, 46.

50 J. D. Miller, *J. Chem. SOC. (A)*, 1968, 1778.

51 M. Mazloum-Ardakani, H. Beitolahli, M. K. Amini, F. Mirkhalaf, B. F. Mirjalili, *Biosens. Bioelectron.*, 2011, **26**, 2102.

52 J. A. Harrison, Z. A. Khan, *J. Electroanal. Chem. Interfacial Electrochem.*, 1970, **28**, 131.

53 T. Buch, *J. Chem. Phys.*, 1965, **43**, 761.

54 J. A. McMillan, B. Smaller, *J. Chem. Phys.*, 1961, **35**, 1698.

55 N. Kanrakl, I. Yasumori, *J. Phys. Chem.*, 1978, **82**, 2351.

56 N. M. Gresley, W. P. Griffith, A. C. Laemmel, H. I. S. Nogueira, *J. Mol. Catal. A: Chem.*, 1997, **117**, 185-198.

57 A. A. Noyes, J. L. Hoard, K. S. Pitzer, *J. Am. Chem. Soc.*, 1935, **57**, 1221.

58 H. N. Po, J. H. Swinehart, T. L. Allen, *Inorg. Chem.*, 1968, **7**, 244.

59 D. M. Yos, *J. Am. Chem. Soc.*, 1926, **47**, 152.

60 L. Yu, J. Wang, D. Guo, W. You, M. Liu, L. Zhang, and C. Li, *Dalton trans.*, submitted. DT-COM-07-2014-002308.

61 A. P. Ginsberg, *Inorganic syntheses*. John Wiley & Sons, 1990, **27**, 100.

62 N. Haraguchi, Y. Okaue, T. Isobe, Y. Matsuda, *Inorg. Chem.*, 1994, **33**, 1015.

63 G. T. Morgan, F. H. Burstall, *Chemical Research Laboratory*, Teddington, Middlesex, 1930, 2594.

64 G. M. Sheldrick, SHELXS97, program for crystal structure solution. University of Gottingen, Germany, 1997.

Cite this: DOI: 10.1039/c0xx00000x

[www.rsc.org/xxxxxx](http://www.rsc.org/xxxxxx)

**ARTICLE TYPE**

## Catalytic Water Oxidation Based on Ag(I)-Substituted Keggin Polyoxotungstophosphate

Ying Cui, Lei Shi, Yanyi Yang, Wansheng You,\* Lancui Zhang, Zaiming Zhu, Meiyang Liu, and Licheng Sun\*

A Ag(I) complex formulated as  $[H_3Ag^I(H_2O)PW_{11}O_{39}]^{3-}$  is formed in aqueous solution. It can be oxidized by  $S_2O_8^{2-}$ , generating a dark green Ag(II) complex  $[H_3Ag^{II}(H_2O)PW_{11}O_{39}]^{2-}$  dominantly and a small amount of Ag(III) complex  $[H_3Ag^{III}OPW_{11}O_{39}]^{3-}$ , and evolving  $O_2$  simultaneously. The rate of  $O_2$  evolution is a first-order law with respect to the concentrations of  $[H_3Ag^I(H_2O)PW_{11}O_{39}]^{3-}$  and  $S_2O_8^{2-}$ , respectively. A possible catalytic water oxidation mechanism of is proposed.

